

# ASCNet: Action Semantic Consistent Learning of Arbitrary Progress Levels for Early Action Prediction

Xiaoli Liu, *Student Member, IEEE*, Di Guo, *Member, IEEE*, and Jianqin Yin, *Member, IEEE*

**Abstract**—Early action prediction aims to recognize human actions from only a part of action execution, which is an important video analysis task for many practical applications. Most prior works treat partial or full videos as a whole, which neglects the semantic consistencies among partial videos of various progress levels due to their large intra-class variances. In contrast, we partition original partial or full videos to form a series of new partial videos and mine the Action Semantic Consistent Knowledge (ASCK) among these new partial videos evolving in arbitrary progress levels. Moreover, a novel Action Semantic Consistent learning network (ASCNet) under the teacher-student framework is proposed for early action prediction. Specifically, we treat partial videos as nodes and their action semantic consistencies as edges. Then we build a bi-directional fully connected graph for the teacher network and a single-directional fully connected graph for the student network to model ASCK among partial videos. The MSE and MMD losses are incorporated as our distillation loss to further transfer the ASCK from the teacher to the student network. Extensive experiments and ablative studies have been conducted, demonstrating the effectiveness of modeling ASCK for early action prediction. With the proposed ASCNet, we have achieved state-of-the-art performance on two benchmarks. The code will be released if the paper is accepted.

**Index Terms**—Action prediction, Teacher-student network, Knowledge distillation, Graph neural network.

## 1 INTRODUCTION

Early action prediction (EAP) is an important task in a series of applications ranging from intelligent surveillance, self-driving to human-robot interaction [1], [2]. Different from traditional action recognition tasks, as shown in Figure 1, the EAP aims to predict the semantic label of ongoing actions very early before the action is completely executed. Due to the limited observations, the action semantics of partial videos are ambiguous, especially at the very early stages. Moreover, although the same action execution with different progress levels of videos shares the same action semantics, there exist diverse feature distributions and large intra-class variations. Therefore, predicting human action very early is particularly challenging due to the limited observations and large intra-class variances in different progress levels.

We assume that the same action semantics have similar feature distributions, and similar distributions of partial videos can be measured by correlations of their features, which is called action semantic consistent modeling. Through pairwise action semantic consistent modeling, we learn similar distributions and their action semantic consistencies with arbitrary progress levels, and we name it Action Semantic Consistent Knowledge (ASCK). Therefore, modeling ASCK among arbitrary partial videos is an intuitive way to learn the similar distributions of their features for alleviating the large intra-class variances of partial videos.

- Xiaoli Liu and Jianqin Yin are the School of Artificial Intelligence of Beijing University of Posts and Telecommunications, No.10 Xitucheng Road, Haidian District, Beijing 100876, China.  
Jianqin Yin is the corresponding author.  
E-mail: Liuxiaoli134@bupt.edu.cn, jqyin@bupt.edu.cn.
- Di Guo is with the Department of Computer Science and Technology of Tsinghua University, Beijing 100084, China.

Manuscript received January 13, 2022; revised January 13, 2022.

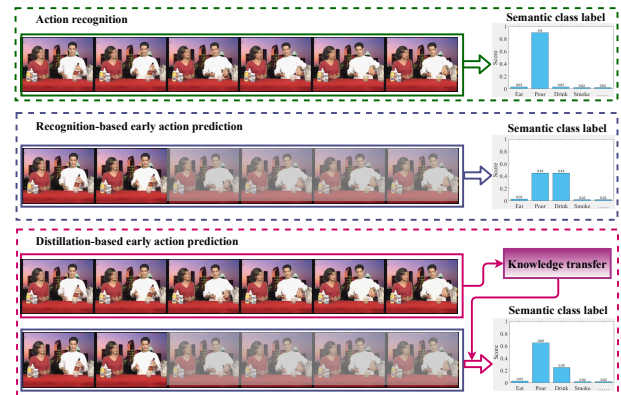


Fig. 1. Action recognition VS early action prediction (EAP). The action recognition model achieves an accurate result of “Pour” from a complete action sequence. The recognition-based EAP model results in ambiguous predictions of “Pour” and “Drink” directly from an incomplete action sequence. The distillation-based EAP model obtains improved results by transferring additional knowledge from the full video.

Many prior works have been proposed for EAP, mainly including recognition-based methods and distillation-based methods. As shown in Figure 1, the recognition-based methods focus on predicting the semantic label of partial videos by capturing the spatiotemporal features of the limited observed sequence with incomplete action executions [3], [4], [5]. For example, Sun et al. [4] proposed a discriminative relational recurrent network (DR2N) to model spatiotemporal interactions between actors of several historical frames for predicting future actions. As shown in the middle of Figure 1, due to limited observations, the partial video shares ambiguous semantics of “Pour” and “Drink”,

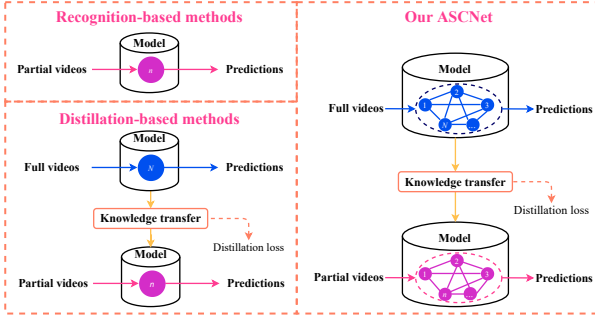


Fig. 2. Different pipelines for early action prediction. The blue dots denote the information from full videos, the pink dots denote the information from partial videos, and the numbers in the dots denote the progress levels of the related videos. The left one denotes two general pipelines for EAP, and the right one shows the pipeline of our ASCNet.

and the recognition-based methods inevitably lead to poor performance. As shown in the bottom of Figure 1, the distillation-based methods try to transfer additional action knowledge from full videos for the missing information of partial videos, which can effectively reduce the ambiguous semantics for predictions [6], [7], [8], [9], [10]. However, as shown in Figure 2, most of the recognition-based or distillation-based methods treat the partial or full videos as a whole, suffering from the limited ability to consider ASCK among partial videos with different progress levels. By contrast, as shown in Figure 4 and Figure 2, we partition original partial or full videos into a series of new partial videos with arbitrary progress levels, and we model ASCK among these new partial videos for predictions.

In this paper, we propose a novel Action Semantic Consistent learning network (ASCNet) under the teacher-student framework for EAP. Specifically, we build the teacher network using a bi-directional fully connected graph with partial videos as nodes. The teacher network distills ASCK among partial videos from lower progress levels to higher progress levels and higher progress levels to lower progress levels. The student network is built with a single-directional fully connected graph since future information is not available during the testing phase. The student network distills ASCK among partial videos from lower progress levels to higher progress levels. We further transfer the ASCK from full to partial videos via layer-wise distillation loss between teacher and student networks. With these elegant designs, the student network also distills ASCK from higher progress levels to lower progress levels for predictions. In contrast to [10], we consider the ASCK among partial videos with arbitrary progress levels instead of adjacent partial videos. We have achieved a new state-of-the-art performance on two benchmarks (i.e., UCF101, HMDB51), showing the effectiveness of modeling ASCK.

Our main contributions are three folds. (1) To the best of our knowledge, we are the first to explore ASCK among partial videos with arbitrary progress levels, which helps to learn similar feature distributions of partial videos with the same action execution for accurate predictions. (2) We propose a novel ASCNet model via the teacher-student framework for EAP. On the one hand, we explore ASCK via the teacher and student networks and distillation loss. On

the other hand, we further transfer ASCK from the teacher to the student to help reduce large intra-class variances for predictions. (3) Experimental results show our new state-of-the-art performance on two datasets, demonstrating the effectiveness of our method. The ablative analysis further shows that modeling ASCK among arbitrary partial videos can effectively improve predictions.

## 2 RELATED WORK

**Early Action prediction.** Most of the exiting works follow the pipeline of action recognition by directly recognizing the semantic label from partial observations [11], [12], [13], [14], [15], [16], [17]. Kong et al. [13] proposed a men-LSTM model to remember the hard-to-predict samples, which forced their model to learn a more complex classified boundary for accurate predictions. Similarly, Li et al. [16] modeled the relationships between the similar action pairs and dynamically marked the hard-predicted similar pairs for 3D skeleton-based EAP. Wu et al. [18] and Yao et al. [19] focused on the interaction relationship modeling and their evolution for EAP. Li et al. [20], [21] mined the temporal sequential patterns via causality of continuing action units, context cue, and action predictability for the long duration action prediction. The recognition-based methods easily suffered from poor performance due to the limited observations and large intra-class variations among partial videos in different progress levels.

Many works struggled to reconstruct missing information of partial videos by predicting future information [7], [8], [22], [23], [24], [25], [26] or distilling action knowledge from the full videos with complete action executions [6], [9], [10]. For example, some works were proposed to jointly learn future motions and relationships between the observed and future information for early predictions [7], [8], [23], [24]. Kong et al. [6] exploited abundant sequential context features from full videos to enrich and reconstruct the features of partial videos. Cai et al. [9] learned feature embeddings by transferring the knowledge between partial and full videos. Wang et al. [10] learned progressive action knowledge between adjacent partial videos but ignored semantic consistencies of partial videos between lower progress levels and higher progress levels, suffering from the limited ability for the large intra-class variations. To sum up, the prior works focused on distilling ASCK (1) between partial videos and full videos via distillation loss (2) or of adjacent partial videos via LSTM (Long Short-Term Memory) cells. By contrast, we consider ASCK among arbitrary partial videos.

**Knowledge distillation.** Knowledge distillation models were mainly achieved via the teacher-student framework by distilling knowledge from a cumbersome teacher network and assisting in learning a lightweight student network for model compression [27], [28]. Recently, Cai et al. [9] and Wang et al. [10] introduced the knowledge distillation model for EAP. These models tried to distill action knowledge from full videos by the teacher network and transferred it to the partial videos by the student network. However, Cai et al. [9] ignored the correlations among different partial or full videos, and Wang et al. [10] focused on the correlations between adjacent partial videos. In contrast to [9] and [10],

we consider the correlations between any partial or full videos and model their ASCK.

**Graph neural network (GNN).** Traditional graph neural networks have been deployed for the non-Euclidean data such as point cloud, human skeleton data [29]. For example, many researchers treated joints of the human body as nodes and their relationships as edges for the skeleton-based action recognition [30], [31] or human motion prediction [32]. Recently, GNNs have been extended to a series of visual tasks [33], [34], [35], [36], [37], [38], [39], [40], [41]. Liu et al. [33] treated the videos as the 3D point clouds for learning video representations. Zhao et al. [40] and Xu et al. [37] took video snippets as nodes and their relationships as edges to exploit the correlations among video snippets for temporal action detection. Similarly, Zeng et al. [39] built an action proposal graph to exploit the relationships between proposals for temporal action detection. Bai et al. [41] proposed a boundary content GNN (BC-GNN) to model the relationships between temporal proposals' boundary and action content. Wang et al. [35] represented the videos as space-time region graphs by treating the object region proposals as nodes for video-based action recognition. Li et al. [36] transformed a video as a graph with each frame as the node, capturing low-level global temporal clues for recognition.

Due to domain gaps of different tasks, these video graphs can not be directly adopted for EAP. In contrast to prior works, we treat the whole partial or full videos as nodes and their semantic consistencies as edges. More differently, the action semantics of all nodes in our graph is the same, completely different from the existing works.

### 3 METHODOLOGY

#### 3.1 Problem formulation

Consistent with the existing works [1], [6], [10], we assume that a video contains the action with complete executions. Given a video  $X$ , we uniformly partition it into  $N$  segments as  $\{x_1, x_2, \dots, x_N\}$ . The first  $n$  segments form a partial video  $X_n = [x_1, x_2, \dots, x_n]$  with a progress level of  $n$ , and its observation ratio is defined as  $n/N$ , which represents the action completion degree. Early action prediction (EAP) can be formulated as equation 1.

$$c_n = f(X_n, n) \quad (1)$$

where  $f(\cdot)$  is a mapping that transforms a partial video  $X_n$  into a semantic label  $c_n$ ,  $n$  denotes the progress level of partial video  $X_n$ , and  $n < N$  for the EAP.

As shown in Figure 2, the distillation-based models utilize full videos to obtain additional information for the missing information of partial videos with incomplete action execution, effectively assisting predictions. Following this pipeline, we build an ASCNet under the teacher-student framework to parameterize  $f(\cdot)$  for predictions in the following sections. In contrast to prior works, we model ASCK among partial videos with arbitrary progress levels and further distill ASCK from the teacher network to the student network, which assists in learning missing information of partial videos to reduce their semantic ambiguity.

#### 3.2 Early action prediction

Figure 3 shows the overall framework of our ASCNet for EAP, which mainly includes three parts: teacher network, student network, and loss. The teacher network learns ASCK of partial videos hidden in the full videos. The ASCK is transferred from the teacher to the student via the distillation loss to enrich the ASCK of partial videos for early predictions. Besides, we utilize the advantages of relational modeling of GNNs to model ASCK among partial videos with arbitrary progress levels. Furthermore, graph generation is the key to building the teacher and student networks. In the following sections, we first show our graph generation. Then, we propose two backbone layers based on the generated graphs. Next, we describe the network structure of ASCNet. Finally, we define our loss to optimize our model.

##### 3.2.1 Graph generation

Consistent with prior works [6], [9], [10], [12], [13], [42], we assume that full videos contain complete action execution, that is to say, the full videos implicitly include partial videos with arbitrary progress levels. Similarly, current partial videos contain partial videos with lower progress levels. Based on the observation above, the original partial or full videos can be partitioned into new partial videos with lower progress levels. In this way, we can conveniently model ASCK of partial videos with different progress levels for predictions.

Generally, the teacher network is applied to full videos, and the student network is applied to partial videos with different progress levels. Therefore, we build a bi-directional fully connected graph for the teacher network, enabling the network to model ASCK among partial videos with arbitrary progress levels. We build a single-directional fully connected graph for the student network since future information is not available during the testing phase, constraining the network to model the ASCK among partial videos from lower progress levels to higher progress levels. As a result, we build two graphs for the teacher and student networks as follows.

As shown in Figure 4, firstly, we partition the original video  $X$  to obtain the new partial videos with different progress levels as defined in section 3.1. Then, we respectively extract motion features for representing the partial videos. Finally, using the features of partial videos as nodes and their semantic consistencies as edges, and two types of graphs are defined for the teacher network and student network, respectively.

**Feature extraction.** Motion features are critical to representing human action. Recently, optical flows have shown their effectiveness in representing motion information in a variety of visual tasks [1], [43]. In this paper, we also follow this pipeline. As described in [45], we also use a pre-trained BN-Inception network [44] on Kinetics-400 dataset [46] to extract the features using optical flow images for experiments. Specifically, we first extract the optical flow images of partial or full videos, respectively. Then, a sliding window with a size of 5 and an overlap of 4 to collect a batch of optical images. The two-directional optical flow images are stacked and resized as a tensor with a size of

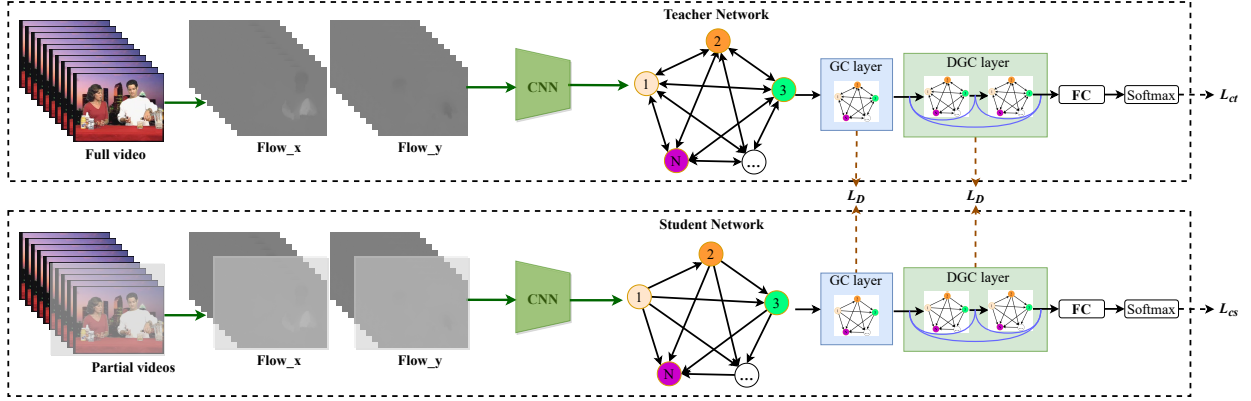


Fig. 3. Overall framework. A novel ASCNet is built under the teacher-student framework for early action prediction.

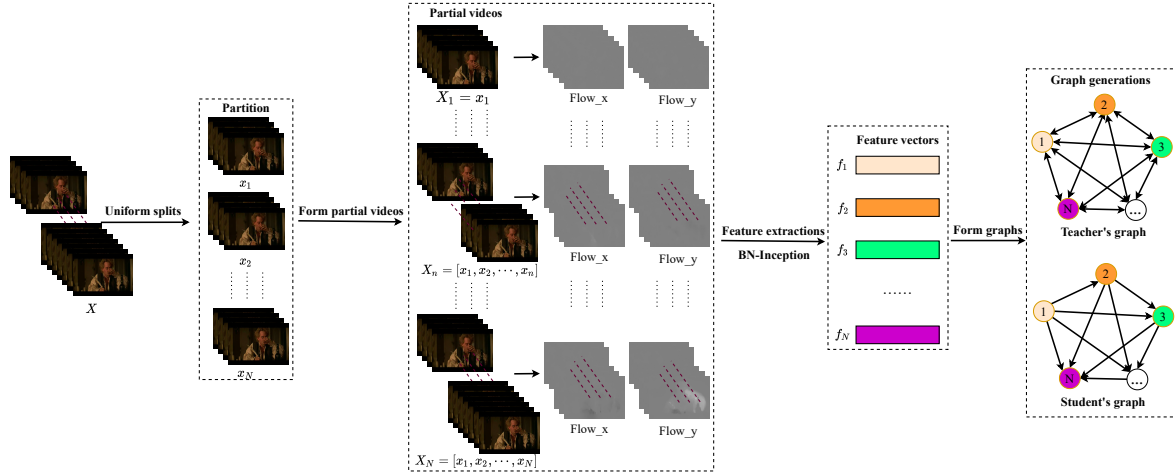


Fig. 4. Graph generation. Given a video  $X$ , we first uniformly split it into  $N$  segments  $\{x_1, x_2, \dots, x_N\}$ . Then, the partial video  $X_n$  with a progress level of  $n$  can be formed by the first  $n$  segments via concatenation along the temporal dimension. Next, we calculate the optical flow of partial videos [43] and apply BN-Inception network [44] to extract their spatiotemporal features using their optical flow images, respectively.  $f_n$  denotes the extracted features of the partial video  $X_n$  ( $n = 1, 2, \dots, N$ ). Finally, two types of graphs are built for the teacher and student networks with the features of partial videos as nodes and their semantic consistencies as edges.

$10 \times 224 \times 224$ . Next, these tensors are set as the input of the BN-Inception network, and we obtain a sequence of feature vectors with a size of  $1 \times D$  (Here,  $D=1024$ ) for each partial or full video. Finally, we apply an average pooling to these feature vectors and obtain the final feature representation with a size of  $1 \times D$  for a partial or full video.

### 3.2.2 Graph convolutional (GC) layer

To model semantic consistencies among partial or full videos, we define a graph convolutional network layer as follows by equation 2.

$$\begin{aligned} F_{l+1} &= GC(F_l) \\ &= A_l F_l W_l \end{aligned} \quad (2)$$

where  $GC(\cdot)$  denotes the defined graph convolutional layer,  $F_l$  denotes a tensor with a shape of  $N \times D_l$  at the  $l$ -th layer, and the  $i$ -th row of the tensor denotes the feature vector of a partial video with a progress level of  $i$  as described in section 3.2.1.  $W_l$  is a learnable weight with a shape of  $D_l \times D_{l+1}$ , and  $D_l$  is the dimension of the  $l$ -th layer.  $A_l$  denotes the adjacent matrix with a shape of  $N \times N$ , and  $N$  denotes the number of progress levels of partial videos.

Instead of simply initializing the adjacent matrix with random weights as done in prior works, we add a constrained matrix to the adjacent matrix by an element-wise multiplication. The constrained matrix is calculated by the cosine similarity between two partial or full videos, encouraging the network to maximize their similarities and model their semantic consistencies. Therefore, our adjacent matrix  $A_l$  can be formulated as follows by equation 3.

$$A_l = M \odot A' \odot S \quad (3)$$

where  $M$  is a binary mask matrix which indicates the indexes of partial videos for distillation.  $A'$  denotes a learnable adjacent matrix as done prior works [32], and  $S$  is a introduced constrained matrix. The shape of  $M$ ,  $A'$  or  $S$  is  $N \times N$ , and  $\odot$  denotes an element-wise multiplication.

The constrained matrix  $S$  is formulated as equation 4.

$$s_{i,j} = \frac{f_i f_j^T}{\|f_i\|_2 \|f_j\|_2} \quad (4)$$

where  $s_{i,j}$  denotes an element of  $S$  at the  $i$ -th row and  $j$ -th column, which can be calculated by the cosine similarity of

partial videos between the  $i$ -th progress level and the  $j$ -th progress level.  $i, j = 1, 2, \dots, N$ .  $f_*$  denotes a feature vector of a partial video with a progress level of  $*$ , i.e., the  $*$ -th low of  $F_l$  in equation 2.  $f^T$  denotes the transpose of matrix  $f$ .

### 3.2.3 Densely graph convolutional block (DGC)

To improve the ability of the model, we build a dense graph convolutional block using the predefined GC layer, formulated by equation 5.

$$\begin{aligned} F_{l+1} &= DGC(F_l) \\ &= g(g(F_l) + F_l) + (g(F_l) + F_l) + F_l \end{aligned} \quad (5)$$

where  $g(\cdot)$  denotes a graph convolutional layer  $GC(\cdot)$  followed by a batch normalization layer  $BN(\cdot)$ , a ReLU layer and a dropout layer  $\delta(\cdot)$ , i.e.,  $g(*) = \delta(BN(GC(*)))$ .

The dense connections enable the network to fuse the low-level features from shallow layers via the element-wise summation, enhancing the features of each partial video to some extent.

### 3.2.4 Network structure

Based on the generated graphs and the predefined backbone layers, we build our ASCNet by the teacher-student framework for EAP, utilizing the ASCK among partial videos with different progress levels.

**Teacher network.** As shown in Figure 3, we apply a bi-directional fully connected graph for the teacher network as described in Section 3.2.1. More specifically, the element values of binary mask matrix  $M$  in equation 3 are set to 1, i.e.  $m_{i,j}=1$ ,  $m_{i,j} \in M$  and  $i, j = 1, 2, \dots, N$ . In this way, the teacher network models ASCK among any partial or full videos from lower progress levels to higher progress levels and higher progress levels to lower progress levels.

The detailed structure of the teacher network is shown in Figure 3, including a GC layer, a DGC layer, a fully connected (FC) layer, and a SoftMax layer, among which the GC and DGC layers are first applied to update the features of nodes and edges of the graph, so as to model the ASCK among different videos with arbitrary progress levels. Then, the FC and SoftMax layers are applied to obtain the semantic labels of videos.

**Student network.** As shown in Figure 3, the student network shares the same structure with the teacher network except for the single-directional graph. Therefore, the binary mask matrix  $M$  in equation 3 is defined by equation 6. In this way, the partial video can not obtain the information from the followed partial videos with higher progress levels. The ASCK is modeled among partial videos from lower progress levels to higher progress levels. Nonetheless, the ASCK from higher progress levels to lower progress levels can be distilled from the teacher network by the distillation loss.

$$m_{i,j} = \begin{cases} 1, & i \geq j \\ 0, & \text{otherwise} \end{cases} \quad (6)$$

where  $m_{i,j} \in M$  and  $i, j = 1, 2, \dots, N$ .

Furthermore, the FC and SoftMax layers of the student model are shared with that of the teacher network, which jointly trains the classifiers for EAP.

### 3.2.5 Loss

We optimize our model using the loss defined in equation 7, which jointly achieves ASCK distillation among partial videos and predicts the semantic label for the videos.

$$L = L_D + L_C \quad (7)$$

$$\begin{aligned} L_D &= L_{MSE} + L_{MMD} \\ &= \sum_{l=1}^M (\|F_{ls} - F_{lt}\|_2 + \|F_{ls}F_{ls}^T - F_{lt}F_{lt}^T\|) \end{aligned} \quad (8)$$

$$\begin{aligned} L_C &= L_{CT} + L_{CS} \\ &= \sum_{i=1}^N (CE(\hat{y}_{it}, y_i) + CE(\hat{y}_{is}, y_i)) \end{aligned} \quad (9)$$

where  $L_D$  denotes the layer-wise knowledge distillation loss built with MSE and MMD loss as done in [10].  $L_C$  denotes the overall classification loss, including a classification loss of the teacher network  $L_{CT}$  and a classification loss of the student network  $L_{CS}$ .  $CE(\cdot)$  denotes the standard cross-entropy loss between the predictions  $\hat{y}_{i*}$  and the groundtruth  $y_i$ , where  $\hat{y}_{is}$  or  $\hat{y}_{it}$  is the prediction of the student or teacher network.

## 4 EXPERIMENTS

In this section, we first describe datasets and implementation details. Then, we briefly introduce the baselines and show the performance of our method. Finally, we conduct extensive experiments to show our contributions.

### 4.1 Datasets and Implementation Details

**Datasets.** (1) UCF101 [47]. UCF101 dataset is collected from YouTube websites in unconstrained environments. It consists of 13320 videos with 101 action classes, including 23 hours of videos. (2) HMDB51 [48]. HMDB51 dataset contains  $\approx 7000$  videos collected from various sources, from movies to YouTube websites. It consists of 51 action classes, and each class has at least 101 videos.

**Implementation Details.** We implement our models using PyTorch [49], and we use SGD [50] with a momentum rate of 0.9 to optimize our models on one GTX 1080Ti GPU. We train 800 epochs on UCF101 and 400 epochs on HMDB51 to choose the best model by the mean accuracy across different progress levels. The learning rate is initialized to 0.0001 and is reduced by a multiplier of 0.95 at the 100-th, 150-th, 250-th, and 350-th epochs, respectively. The batch size is set to 16, and the dropout ratio is set to 0.5. The numbers of channels are set to 512 at the GC and DGC layers. Consistent with the baselines, we use the same training or testing splits on UCF101 and HMDB51 for evaluations. For a fair comparison, we strictly reproduce the results of PTS' in Table 1 according to the paper in [10] using our features except for their optimized strategies and the weights  $w$  in their KD loss since these items have a limited effect on UCF101. The area under the curve (AUC) is used as our metric by calculating the average predictive accuracy over different progress levels, and  $N$  is set to 10 in experiments.

## 4.2 Baselines

To show the effectiveness of our method, we choose several related classical methods as our baselines including three traditional methods, i.e., IBOW [42], DBOW [42], MTSSVM [51], and five methods based on deep neural network, i.e., DeepSCN [6], Mem-LSTM [13], MSRNN [12], PTS [10] and AKT [9], among which AKT [9] and PTS [10] achieve state-of-the-art performance.

## 4.3 Comparison with baselines

**Prediction results on UCF101.** As shown in Table 1, our method consistently outperforms all baselines in terms of AUC. Compared with the traditional methods with hand-crafted features [42], [51], we obtain a significantly improved accuracy by a margin of +13.95% to +39.99%, respectively, demonstrating the effectiveness of our method powerfully. Compared with some typical methods with deep features [6], [12], [13], we also achieve an appreciable performance by a margin of +4.11% to +10.05%. Moreover, Mem-LSTM [13] and MSRNN [12] use two-stream features and pre-train their models on UCF101, which enables their models to obtain the domain action knowledge on UCF101. By contrast, we extract features of partial or full videos by the pre-trained model on Kinetics-400 without fine-tuning on UCF101. In this way, we can not obtain domain-specific knowledge. Nevertheless, we still achieve improved accuracy by an appreciable margin, showing the effectiveness of our method again.

Compared with the methods that also use knowledge distillation [9], [10], we also achieve the best performance in terms of AUC, i.e., +2.96%, +1.72% and +0.34%, respectively. PTS [10] focuses on distilling progressive action knowledge between adjacent partial videos, and AKT [9] focuses on transferring action knowledge from full videos to partial videos by learning the feature embeddings of each progress level and the discriminative action classifier. However, PTS [10] ignores modeling the correlations between lower observation ratios and higher observation ratios, and AKT [9] ignores modeling the correlations among partial videos with different progress levels, leading to their unsatisfactory performance. In contrast to these methods, we consider the ASCK among videos with arbitrary progress levels, including partial or full videos. Firstly, we distill ASCK among partial videos from lower progress levels to higher progress levels and higher progress levels to lower progress levels. Secondly, we further transfer action knowledge from the teacher network to the student network, which enriches the ASCK of partial videos for accurate predictions. The reasons mentioned above make our model possible to obtain superior predictions. Compared with PTS' [10], our improved accuracy is limited, but the GPU memory and Parameters of our model are significantly decreased by  $\approx 3$  and  $\approx 2$  times, respectively.

We further report detailed results with different observation ratios in Figure 5(a). Our method outperforms all baselines for different observation ratios except for the observation ratio of 0.1. The less accurate prediction at 10% may cause by limited observations and further losing appearance information simply using optical flow features.

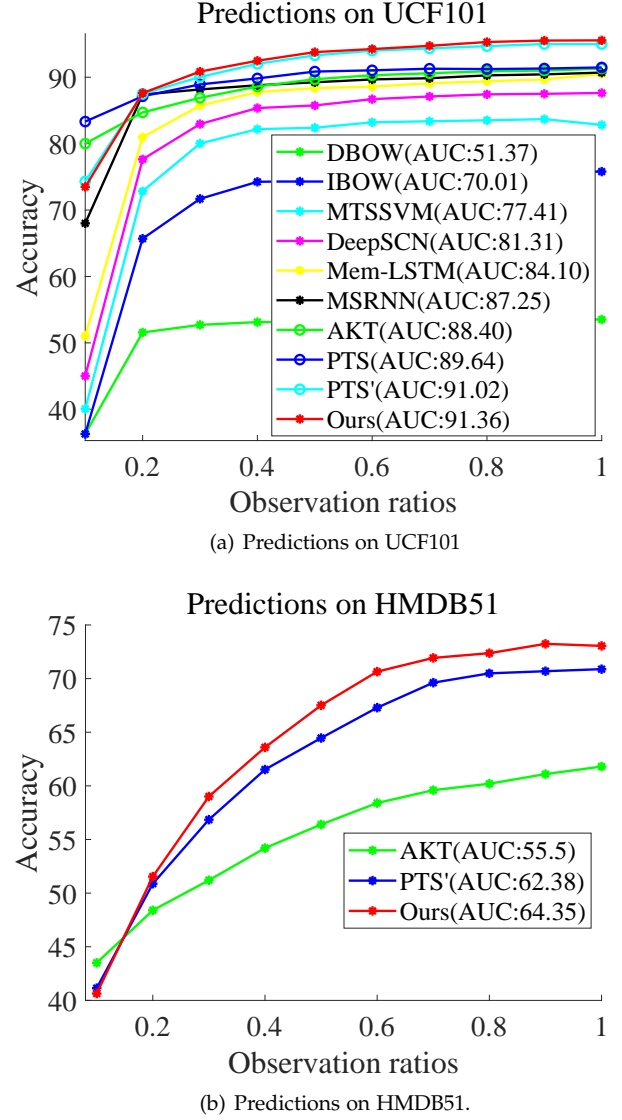


Fig. 5. Prediction results with different observation ratios on UCF101 and HMDB51 datasets. (\*) denotes the performance of the corresponding method in terms of AUC.

**Prediction results on HMDB51.** Compared with the UCF101 dataset, the HMDB51 dataset is more challenging due to more diverse sources and larger intra-class variances, making it more difficult to predict human action very early. As shown in Table 1, compared with AKT [9] and PTS' [10], we achieve superior performance in terms of AUC by a margin of +8.85% and +1.97%, respectively. Although [9] and [10] try to distill action knowledge from full videos, they ignore ASCK among partial videos with different progress levels, especially the semantic consistencies between high progress levels and low progress levels. In contrast, we explicitly model ASCK among partial videos with richer progress levels via the teacher network, the student network, and our distillation loss. The reason may contribute to our superior predictions on the more challenging dataset, strongly showing the importance of explicitly modeling richer ASCK among partial videos for complex activities.

Figure 5(b) shows the detailed results with different

TABLE 1

Prediction results compared with state-of-the-arts. The results for DBOW [42], IBOW [42], MTSSVM [51], DeepSCN [6], Mem-LSTM [13], MSRNN [12] and PTS [10] are reported in [10]. The corresponding results of AKT [9] are also reported in their paper. For a fair comparison, we also reproduce the results of PTS [10] using the same feature with ours, and we name it as PTS'. "+" denotes the improved accuracy of our method compared with the strongest baseline, i.e., PTS' [10], and the bold marks the best results. "2s" denotes "two stream neural network". Moreover, the "GPU Memory" and "Parameters" do not include the feature extraction network.

Method	Features	Pre-trained data	Modality	GPU Memory	Parameters	AUC	
						UCF101	HMDB51
DBOW [42]	STIP	No	RGB	-	-	51.37	-
IBOW [42]	STIP	No	RGB	-	-	70.01	-
MTSSVM [51]	STIP+DT	No	RGB	-	-	77.41	-
DeepSCN [6]	C3D	Sports-1M	RGB	-	-	81.31	-
Mem-LSTM [13]	2s(ResNet-18)	ImageNet+UCF101	RGB+Flow	-	-	84.10	-
MSRNN [12]	2s(VGG)	UCF101	RGB+Flow	-	-	87.25	-
AKT [9]	3D ResNeXt-101	Kinetics-400	RGB	-	-	88.4	55.5
PTS [10]	3D ResNeXt-101	Kinetics-400	RGB	-	-	89.64	-
PTS' [10]	BN-Inception	Kinetics-400	Flow	3303M	5.8M	91.02	62.38
Ours	BN-Inception	Kinetics-400	Flow	<b>861M</b>	<b>2.2M</b>	<b>91.36(+0.34)</b>	<b>64.35(+1.97)</b>

observation ratios on HMDB51. We achieve superior performance by an appreciable margin except for the observation ratio of 0.1. For example, compared with AKT [9] and PTS' [10], we obtain the improved accuracy at the progress level of 2 by **+3.14%** and **+0.66%**, respectively, and our performance is consistently improved at the followed progress levels.

#### 4.4 Ablation analysis

In this section, we conduct extensive experiments to show the effectiveness of our contributions. We show the effectiveness of modeling ASCK via teacher network, student network, and distillation loss, respectively. Then, we evaluate the rationality of the DGC structure.

**Evaluation of modeling ASCK.** As shown in Table 2, the top ones show the effectiveness of distilling ASCK via the teacher and student networks. Compared with our final results, the AUC of "w/o 2dir" decreases by 0.5% and 0.1% on UCF101 and HMDB51, respectively. When we further remove the teacher network, denoting by "Student", the AUC decreases by 1.8% on both UCF101 and HMDB51. The results show the effectiveness of distilling ASCK from full videos. Moreover, compared with "w/o 2dir", the AUC of "Student" decreases by 1.3% and 1.7% on UCF101 and HMDB51, respectively. The single-directional graph by the teacher network still enables the model to distill ASCK from lower progress levels to higher progress levels. Therefore, the teacher network with the single-directional graph also greatly helps to improve the predictions. When we do not consider the ASCK of teacher or student network by setting the adjacent matrixes to the diagonal matrixes (i.e., "Diag  $A_{ls}$ ", "Diag  $A_{lt}$ ", and "Diag  $A_l$ "), the performance consistently decreases, showing the effectiveness of modeling ASCK. Moreover, "Diag  $A_{ls}$ " obtains the worst results, showing the effectiveness of utilizing the semantic consistencies of partial videos with lower progress levels by the student network.

Compared with "w/o  $L_D$ ", the AUC of our model increases by 2.0% and 2.8% on UCF101 and HMDB51, respectively. When we remove the MMD loss  $L_{MMD}$  from the distillation loss  $L_D$ , the accuracy decreases by 0.8% and 1.5% on UCF101 and HMDB51, respectively. When

TABLE 2

Results of ablative studies. "w/o 2dir" denotes a single graph for the teacher network, "Diag  $A_{l*}$ " denotes that the adjacent matrix shown in equation 2 of the teacher/student network is a diagonal matrix, "Student" denotes only the student network without the teacher network in Figure 3, "w/o  $L_D$ " denotes without the  $L_D$  loss in equation 7, "w/o  $L_{MMD}$ " denotes MSE loss without MMD loss in  $L_D$ , "w/o  $L_{MSE}$ " denotes the MMD loss without MSE loss in  $L_D$ , and "w/o DC" denotes the block without densely residual connections in the DCG block. The bold marks the best results, "(-\*)" shows the decreased accuracy compared with our final results, and the AUC denotes the average prediction overall 10 progress levels.

Model	AUC	
	UCF101	HMDB51
w/o 2dir	90.9 (-0.5)	64.3 (-0.1)
Diag $A_{ls}$	90.2 (-1.2)	63.5 (-0.9)
Diag $A_{lt}$	91.0 (-0.4)	63.9 (-0.5)
Diag $A_l$	91.0 (-0.4)	63.7 (-0.7)
Student	89.6 (-1.8)	62.6 (-1.8)
w/o $L_D$	89.4 (-2.0)	61.6 (-2.8)
w/o $L_{MMD}$	90.6 (-0.8)	62.9 (-1.5)
w/o $L_{MSE}$	91.1 (-0.3)	64.1 (-0.3)
w/o DC	90.2 (-1.2)	63.1 (-1.3)
<b>Ours</b>	<b>91.4</b>	<b>64.4</b>

we remove the MSE loss  $L_{MSE}$  from the distillation loss  $L_D$ , the accuracy decreases by 0.3% on both UCF101 and HMDB51. These results reveal the following conclusions. (1) Incorporating both MSE and MMD loss for the distillation of ASCK from the full video is of great help to improve the predictions. (2) Compared with the MMD loss, MSE contributes more to the distillation, but MMD can further improve the distillation. This proves that MSE and MMD losses are complementary for knowledge distillation.

Figure 6 show the detailed results with different progress levels on UCF101 and HMDB51. The improved results on UCF101 are consistent with that of HMDB51, consistently showing the effectiveness of ASCK distillation via both the design of network structure and the distillation loss.

**Evaluation of the rationality of DGC structure.** "w/o DC" denotes without densely residual connections in DGC block. As shown in Table 2, compared with "w/o DC", the accuracy of our method increases by 1.2% and 1.3% on UCF101 and HMDB51, respectively. The results show

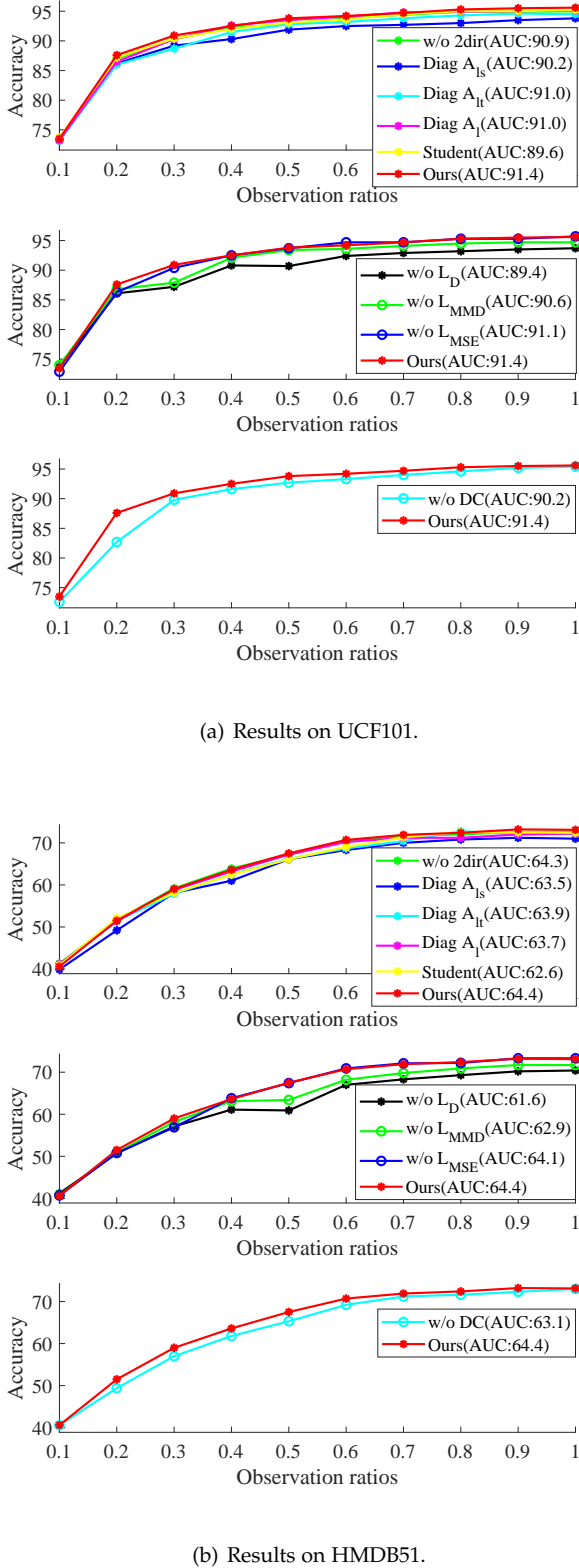


Fig. 6. Detailed results of ablation studies. (\*) denotes the performance of the corresponding method in terms of AUC.

the effectiveness of the densely residual connections on leveraging low-level features for accurate predictions. The detailed results in Figure 6 also show similar improved

results. Therefore, the results in Table 2 and Figure 6 consistently show the rationality of DGC structure.

## 5 CONCLUSION

In this paper, we propose a novel ASCNet model by a teacher-student framework, utilizing the relational modeling of GNNs to model ASCK of partial videos with arbitrary progress levels. Specifically, we build a bi-directional and a single-directional fully connected graph for the teacher and student networks, respectively. The teacher network with the bi-directional graph considers ASCK of partial videos with arbitrary progress levels. The student network with the single-directional graph captures ASCK among partial videos from lower progress levels to higher progress levels. Also, it enriches their ASCK from the teacher network via distillation loss. In contrast to prior works, we consider ASCK among arbitrary partial videos and distill ASCK by the teacher and student networks and distillation loss. Extensive experiments have shown the effectiveness of explicitly modeling ASCK for predictions. However, due to the missing appearance features using optical flow images, the prediction of 10% is unsatisfactory, which we will investigate in the future.

## ACKNOWLEDGMENTS

This work was supported partly by the National Natural Science Foundation of China (Grant No. 62173045, 61673192), partly supported by the Fundamental Research Funds for the Central Universities(Grant No. 2020XD-A04-2), and partly supported by BUPT Excellent Ph.D. Students Foundation (CX2021314).

## REFERENCES

- [1] H. Zhao and R. P. Wildes, "Review of video predictive understanding: Early action recognition and future action prediction," *arXiv preprint arXiv:2107.05140*, 2021.
- [2] Y. Kong and Y. Fu, "Human action recognition and prediction: A survey," *arXiv preprint arXiv:1806.11230*, 2018.
- [3] L. Chen, J. Lu, Z. Song, and J. Zhou, "Part-activated deep reinforcement learning for action prediction," in *Proceedings of the European Conference on Computer Vision (ECCV)*, 2018, pp. 421–436.
- [4] C. Sun, A. Shrivastava, C. Vondrick, R. Sukthankar, K. Murphy, and C. Schmid, "Relational action forecasting," in *Proceedings of the IEEE Conference on Computer Vision and Pattern Recognition (CVPR)*, 2019, pp. 273–283.
- [5] J. Liu, A. Shahroudy, G. Wang, L.-Y. Duan, and A. C. Kot, "Ssnet: scale selection network for online 3d action prediction," in *Proceedings of the IEEE Conference on Computer Vision and Pattern Recognition (CVPR)*, 2018, pp. 8349–8358.
- [6] Y. Kong, Z. Tao, and Y. Fu, "Deep sequential context networks for action prediction," in *Proceedings of the IEEE Conference on Computer Vision and Pattern Recognition (CVPR)*, 2017, pp. 1473–1481.
- [7] J. Guan, Y. Yuan, K. M. Kitani, and N. Rhinehart, "Generative hybrid representations for activity forecasting with no-regret learning," in *Proceedings of the IEEE Conference on Computer Vision and Pattern Recognition (CVPR)*, 2020, pp. 173–182.
- [8] H. Gammulle, S. Denman, S. Sridharan, and C. Fookes, "Predicting the future: A jointly learnt model for action anticipation," in *Proceedings of the IEEE International Conference on Computer Vision (ICCV)*, 2019, pp. 5562–5571.
- [9] Y. Cai, H. Li, J.-F. Hu, and W.-S. Zheng, "Action knowledge transfer for action prediction with partial videos," in *Proceedings of the AAAI Conference on Artificial Intelligence (AAAI)*, vol. 33, no. 01, 2019, pp. 8118–8125.

- [10] X. Wang, J.-F. Hu, J.-H. Lai, J. Zhang, and W.-S. Zheng, "Progressive teacher-student learning for early action prediction," in *Proceedings of the IEEE Conference on Computer Vision and Pattern Recognition (CVPR)*, 2019, pp. 3556–3565.
- [11] J.-F. Hu, W.-S. Zheng, L. Ma, G. Wang, and J. Lai, "Real-time rgb-d activity prediction by soft regression," in *Proceedings of the European Conference on Computer Vision (ECCV)*. Springer, 2016, pp. 280–296.
- [12] J.-F. Hu, W.-S. Zheng, L. Ma, G. Wang, J. Lai, and J. Zhang, "Early action prediction by soft regression," *IEEE Transactions on Pattern Analysis and Machine Intelligence (TPAMI)*, vol. 41, no. 11, pp. 2568–2583, 2018.
- [13] Y. Kong, S. Gao, B. Sun, and Y. Fu, "Action prediction from videos via memorizing hard-to-predict samples," in *Proceedings of the AAAI Conference on Artificial Intelligence (AAAI)*, vol. 32, no. 1, 2018.
- [14] Y. Kong and Y. Fu, "Max-margin action prediction machine," *IEEE Transactions on Pattern Analysis and Machine Intelligence (TPAMI)*, vol. 38, no. 9, pp. 1844–1858, 2015.
- [15] S. Lai, W.-S. Zheng, J.-F. Hu, and J. Zhang, "Global-local temporal saliency action prediction," *IEEE Transactions on Image Processing (TIP)*, vol. 27, no. 5, pp. 2272–2285, 2017.
- [16] T. Li, J. Liu, W. Zhang, and L. Duan, "Hard-net: Hardness-aware discrimination network for 3d early activity prediction," in *Proceedings of the European Conference on Computer Vision (ECCV)*. Springer, 2020, pp. 420–436.
- [17] Q. Ke, M. Bennamoun, H. Rahmani, S. An, F. Sohel, and F. Boussaid, "Learning latent global network for skeleton-based action prediction," *IEEE Transactions on Image Processing (TIP)*, vol. 29, pp. 959–970, 2019.
- [18] X. Wu, R. Wang, J. Hou, H. Lin, and J. Luo, "Spatial-temporal relation reasoning for action prediction in videos," *International Journal of Computer Vision (IJCV)*, vol. 129, no. 5, pp. 1484–1505, 2021.
- [19] T. Yao, M. Wang, B. Ni, H. Wei, and X. Yang, "Multiple granularity group interaction prediction," in *Proceedings of the IEEE Conference on Computer Vision and Pattern Recognition (CVPR)*, 2018, pp. 2246–2254.
- [20] K. Li, J. Hu, and Y. Fu, "Modeling complex temporal composition of actionlets for activity prediction," in *Proceedings of the European Conference on Computer Vision (ECCV)*. Springer, 2012, pp. 286–299.
- [21] K. Li and Y. Fu, "Prediction of human activity by discovering temporal sequence patterns," *IEEE Transactions on Pattern Analysis and Machine Intelligence (TPAMI)*, vol. 36, no. 8, pp. 1644–1657, 2014.
- [22] Y. Shi, B. Fernando, and R. Hartley, "Action anticipation with rbf kernelized feature mapping rnn," in *Proceedings of the European Conference on Computer Vision (ECCV)*, 2018, pp. 301–317.
- [23] B. Fernando and S. Herath, "Anticipating human actions by correlating past with the future with jaccard similarity measures," in *Proceedings of the IEEE Conference on Computer Vision and Pattern Recognition (CVPR)*, 2021, pp. 13224–13233.
- [24] G. Pang, X. Wang, J. Hu, Q. Zhang, and W.-S. Zheng, "Dbdnet: Learning bi-directional dynamics for early action prediction," in *International Joint Conference on Artificial Intelligence (IJCAI)*, 2019, pp. 897–903.
- [25] Z. Xu, L. Qing, and J. Miao, "Activity auto-completion: Predicting human activities from partial videos," in *Proceedings of the IEEE International Conference on Computer Vision (ICCV)*, 2015, pp. 3191–3199.
- [26] Y. B. Ng and B. Fernando, "Forecasting future action sequences with attention: a new approach to weakly supervised action forecasting," *IEEE Transactions on Image Processing (TIP)*, vol. 29, pp. 8880–8891, 2020.
- [27] J. Gou, B. Yu, S. J. Maybank, and D. Tao, "Knowledge distillation: A survey," *International Journal of Computer Vision (IJCV)*, vol. 129, no. 6, pp. 1789–1819, 2021.
- [28] G. Hinton, O. Vinyals, and J. Dean, "Distilling the knowledge in a neural network," *arXiv preprint arXiv:1503.02531*, 2015.
- [29] Z. Wu, S. Pan, F. Chen, G. Long, C. Zhang, and S. Y. Philip, "A comprehensive survey on graph neural networks," *IEEE Transactions on Neural Networks and Learning Systems (TNNLS)*, vol. 32, no. 1, pp. 4–24, 2020.
- [30] S. Yan, Y. Xiong, and D. Lin, "Spatial temporal graph convolutional networks for skeleton-based action recognition," in *The AAAI Conference on Artificial Intelligence (AAAI)*, 2018.
- [31] K. Cheng, Y. Zhang, X. He, W. Chen, J. Cheng, and H. Lu, "Skeleton-based action recognition with shift graph convolutional network," in *Proceedings of the IEEE Conference on Computer Vision and Pattern Recognition (CVPR)*, 2020, pp. 183–192.
- [32] W. Mao, M. Liu, M. Salzmann, and H. Li, "Learning trajectory dependencies for human motion prediction," in *Proceedings of the IEEE International Conference on Computer Vision (ICCV)*, 2019, pp. 9489–9497.
- [33] X. Liu, J.-Y. Lee, and H. Jin, "Learning video representations from correspondence proposals," in *Proceedings of the IEEE Conference on Computer Vision and Pattern Recognition (CVPR)*, 2019, pp. 4273–4281.
- [34] Y. Chen, M. Rohrbach, Z. Yan, Y. Shuicheng, J. Feng, and Y. Kalantidis, "Graph-based global reasoning networks," in *Proceedings of the IEEE Conference on Computer Vision and Pattern Recognition (CVPR)*, 2019, pp. 433–442.
- [35] X. Wang and A. Gupta, "Videos as space-time region graphs," in *Proceedings of the European Conference on Computer Vision (ECCV)*, 2018, pp. 399–417.
- [36] R.-C. Li, T. Xu, X.-J. Wu, and J. Kittler, "Video is graph: Structured graph module for video action recognition," *arXiv preprint arXiv:2110.05904*, 2021.
- [37] M. Xu, C. Zhao, D. S. Rojas, A. Thabet, and B. Ghanem, "G-tad: Sub-graph localization for temporal action detection," in *Proceedings of the IEEE Conference on Computer Vision and Pattern Recognition (CVPR)*, 2020, pp. 10156–10165.
- [38] Y. Yuan, X. Liang, X. Wang, D.-Y. Yeung, and A. Gupta, "Temporal dynamic graph lstm for action-driven video object detection," in *Proceedings of the IEEE International Conference on Computer Vision (ICCV)*, 2017, pp. 1801–1810.
- [39] R. Zeng, W. Huang, M. Tan, Y. Rong, P. Zhao, J. Huang, and C. Gan, "Graph convolutional networks for temporal action localization," in *Proceedings of the IEEE International Conference on Computer Vision (ICCV)*, 2019, pp. 7094–7103.
- [40] C. Zhao, A. K. Thabet, and B. Ghanem, "Video self-stitching graph network for temporal action localization," in *Proceedings of the IEEE International Conference on Computer Vision (ICCV)*, 2021, pp. 13658–13667.
- [41] Y. Bai, Y. Wang, Y. Tong, Y. Yang, Q. Liu, and J. Liu, "Boundary content graph neural network for temporal action proposal generation," in *Proceedings of the European Conference on Computer Vision (ECCV)*. Springer, 2020, pp. 121–137.
- [42] M. S. Ryoo, "Human activity prediction: Early recognition of ongoing activities from streaming videos," in *Proceedings of the IEEE International Conference on Computer Vision (ICCV)*. IEEE, 2011, pp. 1036–1043.
- [43] L. Wang, Y. Xiong, Z. Wang, Y. Qiao, D. Lin, X. Tang, and L. Van Gool, "Temporal segment networks: Towards good practices for deep action recognition," in *Proceedings of the European Conference on Computer Vision (ECCV)*. Springer, 2016, pp. 20–36.
- [44] S. Ioffe and C. Szegedy, "Batch normalization: Accelerating deep network training by reducing internal covariate shift," in *International Conference on Machine Learning (ICML)*. PMLR, 2015, pp. 448–456.
- [45] J. Yin, X. Liu, F. Sun, H. Liu, Z. Liu, B. Wang, J. Liu, and Y. Yin, "One-shot sadi-epc: a visual framework of event progress estimation," *IEEE Transactions on Circuits and Systems for Video Technology (TCSVT)*, vol. 29, no. 6, pp. 1659–1671, 2018.
- [46] W. Kay, J. Carreira, K. Simonyan, B. Zhang, C. Hillier, S. Vijayanarasimhan, F. Viola, T. Green, T. Back, P. Natsev *et al.*, "The kinetics human action video dataset," *arXiv preprint arXiv:1705.06950*, 2017.
- [47] K. Soomro, A. R. Zamir, and M. Shah, "Ucf101: A dataset of 101 human actions classes from videos in the wild," *arXiv preprint arXiv:1212.0402*, 2012.
- [48] H. Kuehne, H. Jhuang, E. Garrote, T. Poggio, and T. Serre, "Hmdb: a large video database for human motion recognition," in *Proceedings of the IEEE International Conference on Computer Vision (ICCV)*. IEEE, 2011, pp. 2556–2563.
- [49] A. Paszke, S. Gross, S. Chintala, G. Chanan, E. Yang, Z. DeVito, Z. Lin, A. Desmaison, L. Antiga, and A. Lerer, "Automatic differentiation in pytorch," in *Workshop on Neural Information Processing Systems (NIPS-W)*, 2017.
- [50] L. Bottou, "Large-scale machine learning with stochastic gradient descent," in *Proceedings of COMPSTAT'2010*. Springer, 2010, pp. 177–186.

- [51] W. Xu, J. Yu, Z. Miao, L. Wan, and Q. Ji, "Prediction-cgan: Human action prediction with conditional generative adversarial networks," in *Proceedings of the 27th ACM International Conference on Multimedia (ACMMM)*, 2019, pp. 611–619.